Supplementary Data and Information

Multi-curvature micropatterns unveil distinct calcium and mitochondrial dynamics in neuronal networks

Hammad Khan[a], Connor Beck[a], Anja Kunze[*a,b]

[a]Department of Electrical and Computer Engineering, Montana State University, Bozeman, Montana 59717, USA. Email: anja.kunze@montana.edu
[b]Montana Nanotechnology Facility, Montana State University, Bozeman, Montana 59717, USA.

Abstract
This document contains further details about the main article named above. Furthermore, additional graphs and raw data are presented to support the results described in the main article. This document contains six figures S1 – S6 and one supplementary video file V1.

Fine-tuning agarose barrier properties.
Agarose is a highly tunable natural hydrogel that is inert to cellular adhesion and is commonly used to establish *in vitro* cell-to-cell systems[1, 2]. A variety of micro-scaled techniques exist to partition hydrogel structures based on microfluidics or microprinting[2, 3]. In these hydrogel structures, cells can be embedded or repelled. Here we used agarose hydrogels to maximize the parallel design of multi-curvatures for bent neurite network growth in a confined spatial area. For our micropatterns, the agarose hydrogel concentration had to be chosen high enough to prevent the cross growth of neurites through the porous hydrogel barrier but not too viscous to facilitate micropatterning. To achieve this goal, we tested four different agarose gel concentrations (% w/v) against a control (0% w/v = no agarose hydrogel). Agarose powder was dissolved in phosphate-buffered saline (PBS) and autoclaved before dropwise addition to a poly-D-lysine (PDL)-coated polystyrene surface. The agarose drops were immediately gelled over a cooling plate. Cell culture media was applied to the Petri dishes to wash out the PBS solution before neuronal cell bodies were seeded randomly over the surface. Figure S1a shows representative phase contrast and fluorescent images of inhibited neurite growth into the 3% (w/v) agarose area from four different locations in the dish. The agarose hydrogel was spiked with fluorescent beads for visualization purposes. Figure S2b shows the average neurite outgrowth of traced neurites entering the hydrogel area. The length was measured from the liquid/gel barrier until the axonal/neurite tip. While an agarose concentration of 2% (w/v) was sufficient to significantly reduce neurite growth into the hydrogel region below 50 µm, only 3% (w/v) agarose kept the neurite length consistently below 25 µm. The latter depth is important due to the barrier dimensions in the multi-curvature design.

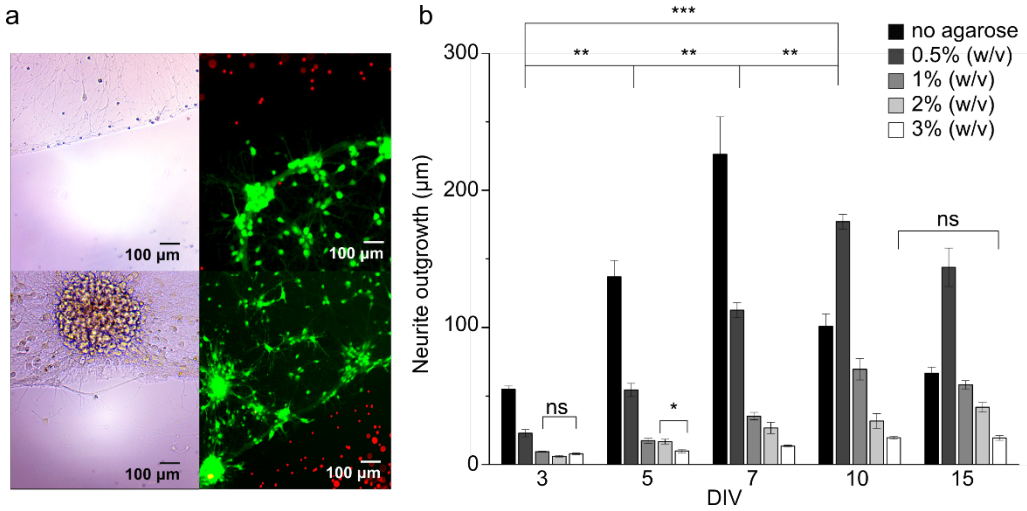

Figure S1: Tunable agarose concentrations modulate neurite outgrowth. (a) Representative images of inert agarose behavior to neuronal cell growth and neurite network formation. Cultured cortical neurons (rat, E18) were seeded adjacent to bead-enriched agarose areas (3% (w/v) and grown for 15 days *in vitro* (DIV). Neurite outgrowth was traced using the FIJI neurite tracer plugin. (b) Bar plots of traced neurite length grown into the hydrogel area for four different agarose concentrations. Significance is indicated based on three different levels: (i) * = $p<0.01$, ** = $p<0.001$, *** = $p<0.0001$ (two-way ANOVA).

Analyzing agarose swelling characteristics.

To test the long-term robustness of the agarose features, we spiked fluorescent microparticles into the agarose hydrogel and monitored their displacement during incubation in Neurobasal culture media every 10 min over 48 h. Using particle image velocimetry, we determined the amount of swelling in the agarose hydrogel (3% (w/v) based on bead displacement. Molten agarose solutions were loaded with fluorescent microparticles (Bangs Lab, 15 µm, Fig. S2 a). Hydrogel patterns were submerged in standard cell culture media (98% (v/v) Neurobasal Plus without Phenol Red, 2% (v/v) B27 Plus Supplement with, Gibco) before imaging. Video recordings were done using a high-resolution inverting microscope (Leica DMi8S) set to a red fluorescent channel. Sampled video sets were exported as an image stack, post-processed, and analyzed using ImageJ. From here, we implemented particle image velocimetry (PIV) using MATLAB PIV (Fig. S2 b) to track particle displacement to assess potential agarose swelling (Fig. S2c). To briefly summarize, PIV works to analyze particle or pattern movement, particularly regarding in-depth analysis and evaluation of measurement accuracy. The program accounts for sensitive computational details such as image pre-conditioning, image correlation, subpixel peak estimators, and data interpolation. For the parameters of our experiment, we implemented a contrast limited adaptive histogram equalizer (CLAHE) to enhance the visibility of nanoparticle fluorescence. An intensity high-pass filter was used to eliminate any background noise in the video and block low-frequency noise during post-processing. Throughout 48 h, spatial displacement of beads in relation to their initial position (x0,y0, at t=0 h) was observed to be below 1.5 µm in all directions within the 10 min time gaps, which is below 10% with the bead diameter (Fig. S2d). Based on diffusion beads may shift their position up to 40% of their diameter. Furthermore, the average bead displacement reduced over time and showed no differences between 24 h and 48 h (Fig. S2e). Hence our hydrogel mixture has shown stable encapsulation of the microbeads and hence seem robust enough to provide a mechanically stable barrier for neuronal cell growth in between the hydrogel barriers over 48 h.

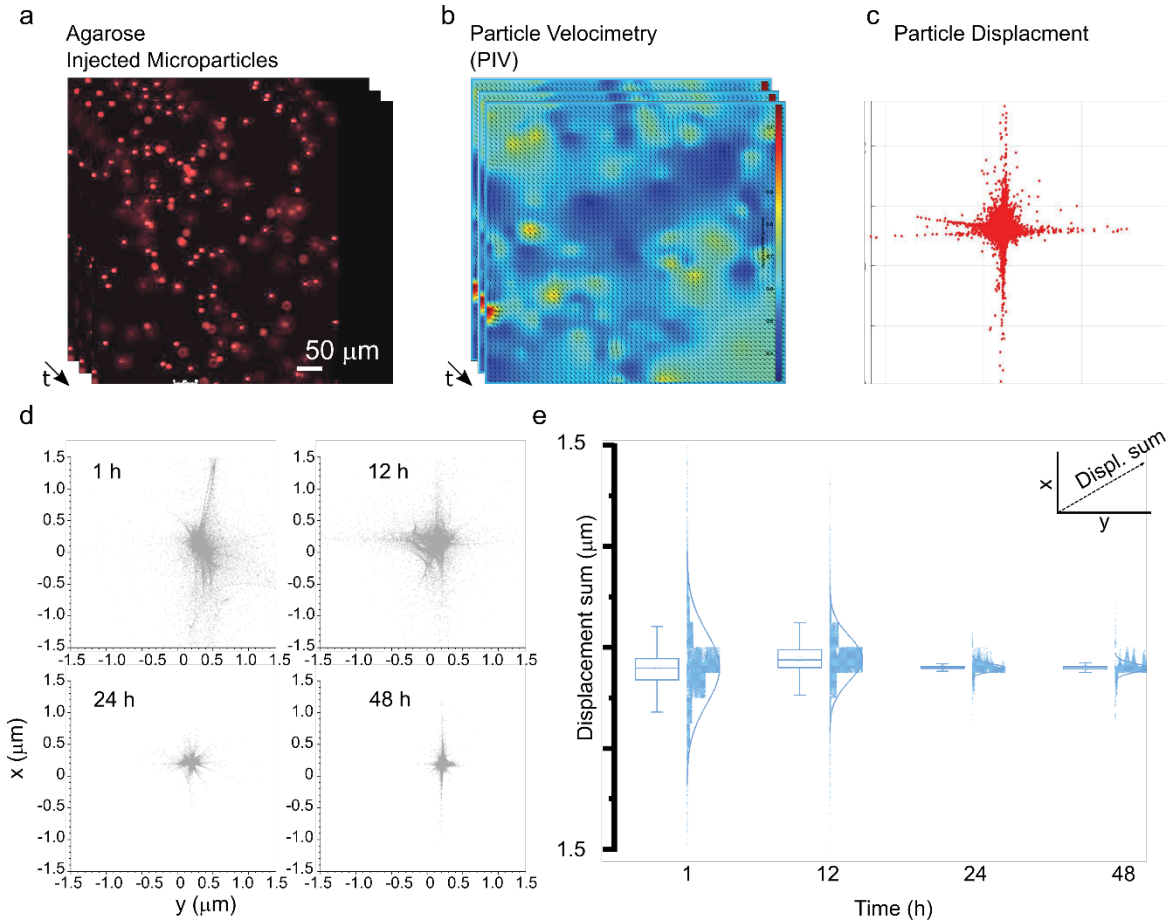

Figure S2: Digital particle image velocimetry implementation gives insight on agarose swelling and stability. (a) Fluorescent microparticles were injected into agarose and micropatterned with the hydrogel for visualization. (b) Using Particle image velocimetry (PIV, MATLAB), bead displacement was quantified. (c) Spatial raster sum plots show accumulated particle displacement over 48 h, where the dot points towards the total displacement. (d) Spatial raster sum plots show individual particle displacement after 1 h, 12 h, 24 h, and 48 h incubation time in the neuronal cell culture medium. (e) The boxplots show the projected displacement sum vector for all tracked particles per sample.

Assessing hydrogel micro pattern robustness during neurite network formation.

The forces assumed here to play a role during neurite network formation may interfere with the micropatterned hydrogel barriers. Periodic imaging was done during neuronal culture to check the neurite growth and intactness of the agarose micropatterned features beyond the 48 h based on differential interference contrast (DIC) microscopy tested in Figure S2. Figure S3 shows mostly undisturbed formation of micropatterned structures over the neuronal cell growth period of two weeks and intact hydrogel barrier features.

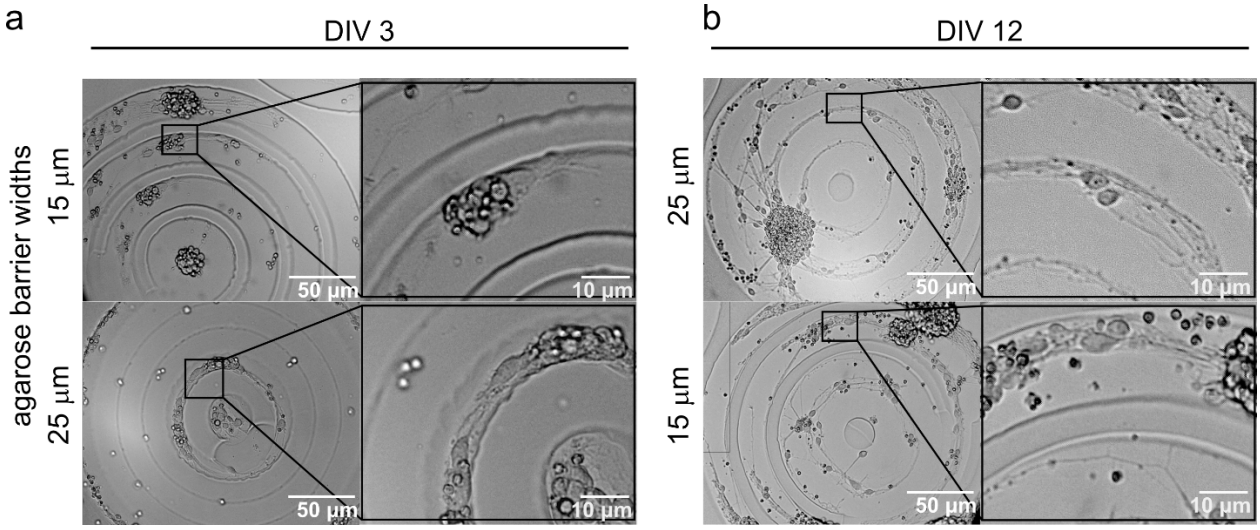

Figure S3: DIC images of micropatterned neuronal cell growth (E18, rat, cortex) in the multi-curvature agarose grooves at (a) 3 da*ys in vitro* (DIV) and at (b) 12 DIV for 25 µm (top row) and 15 µm (bottom row) barrier widths.

Image processing workflow to obtain normalized static calcium fluorescence plots

Several regions of interest (ROI) were captured to account for variability in cell seeding density and fluorescent probe sensitivity for each multi-curvature pattern. The resulting static fluorescent profiles are shown in Figure S4. These profiles provide additional details for the image processing method used in our study.

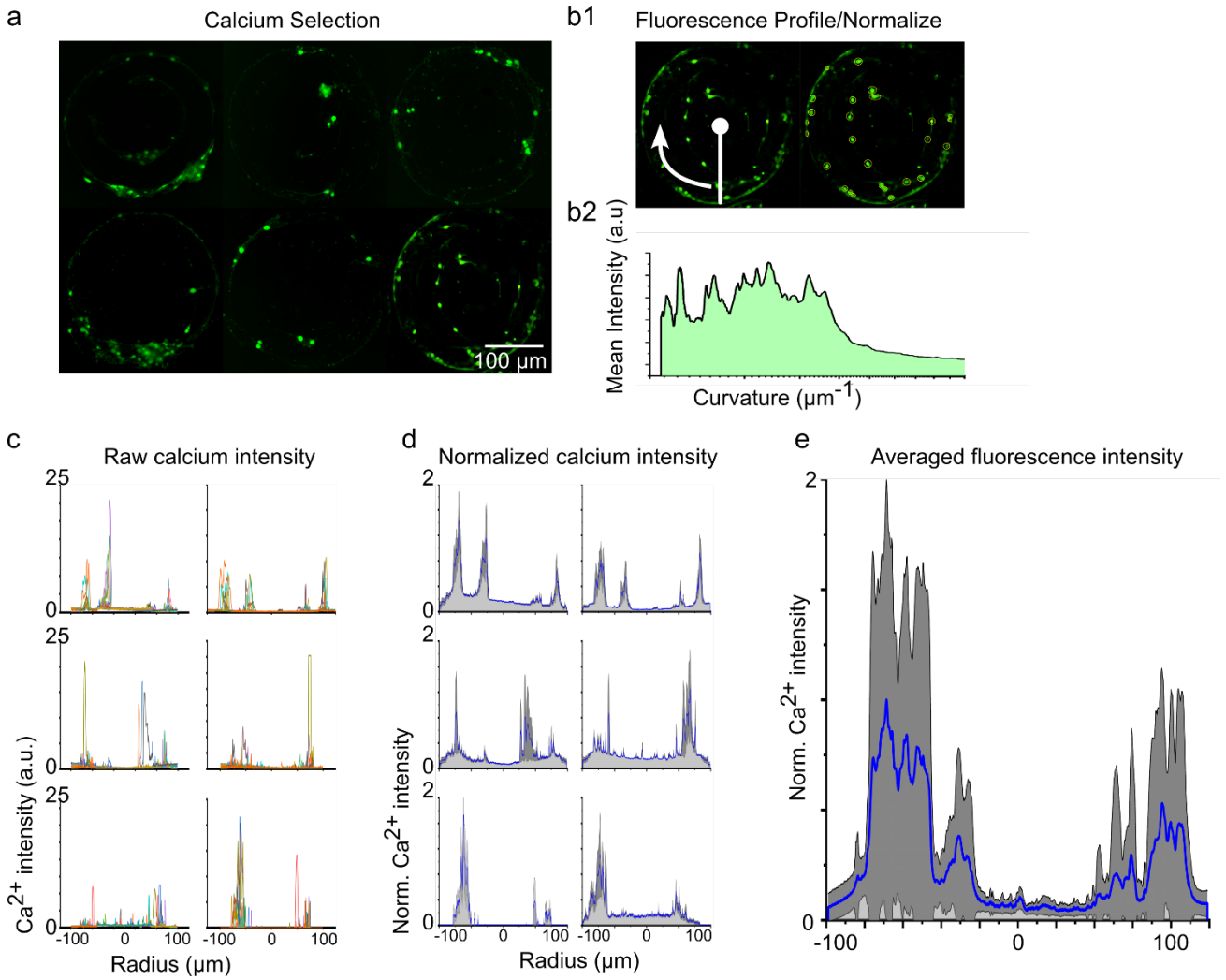

Figure S4: Static calcium (Ca^{2+}) fluorometry for a single multi-curvature pattern. (a) False-color fluorescent image shows a representative sample set of calcium-labeled (Fluo4 AM) neuronal cell growth in the multi-curvature patterns. (b1) A custom semi-automatic script acquires raw fluorescent intensity profiles circulating clockwise through the pattern. (b2) Extracted raw fluorescent intensity profiles showing the mean of all collected surface profiles. (c) Extracted raw mean intensity profiles from six individual patterns of the same topography (15 µm agarose barrier width, 10 µm groove width = curvature region). Intensity values are based on an 8-bit scale (0-255). (d) Normalized calcium intensity plots based on cell count per curvature region and mean intensity. (e) Averaged calcium intensity profiles for the six selected topographically identical micro curvature patterns.

Image processing workflow to obtain temporal calcium dynamics

The comparison of transient calcium activity depending on distinct curvature regions is based on a step-by-step image stack analysis shown in Figure S5. Based on "synchronous" occurrence of calcium events inspired by Ikegaya *et al.*[4] within a time interval of one second, we assume that these neuronal bodies are connected or strongly correlated. Synchronous calcium events have been determined spike raster plots denoting a local increase in cytosolic calcium levels. The resulting spike trains were then time-vise compared through the Sørensen–Dice similarity coefficient to determine synchronous event activity, a previously used metric by Beck *et al.*[5]

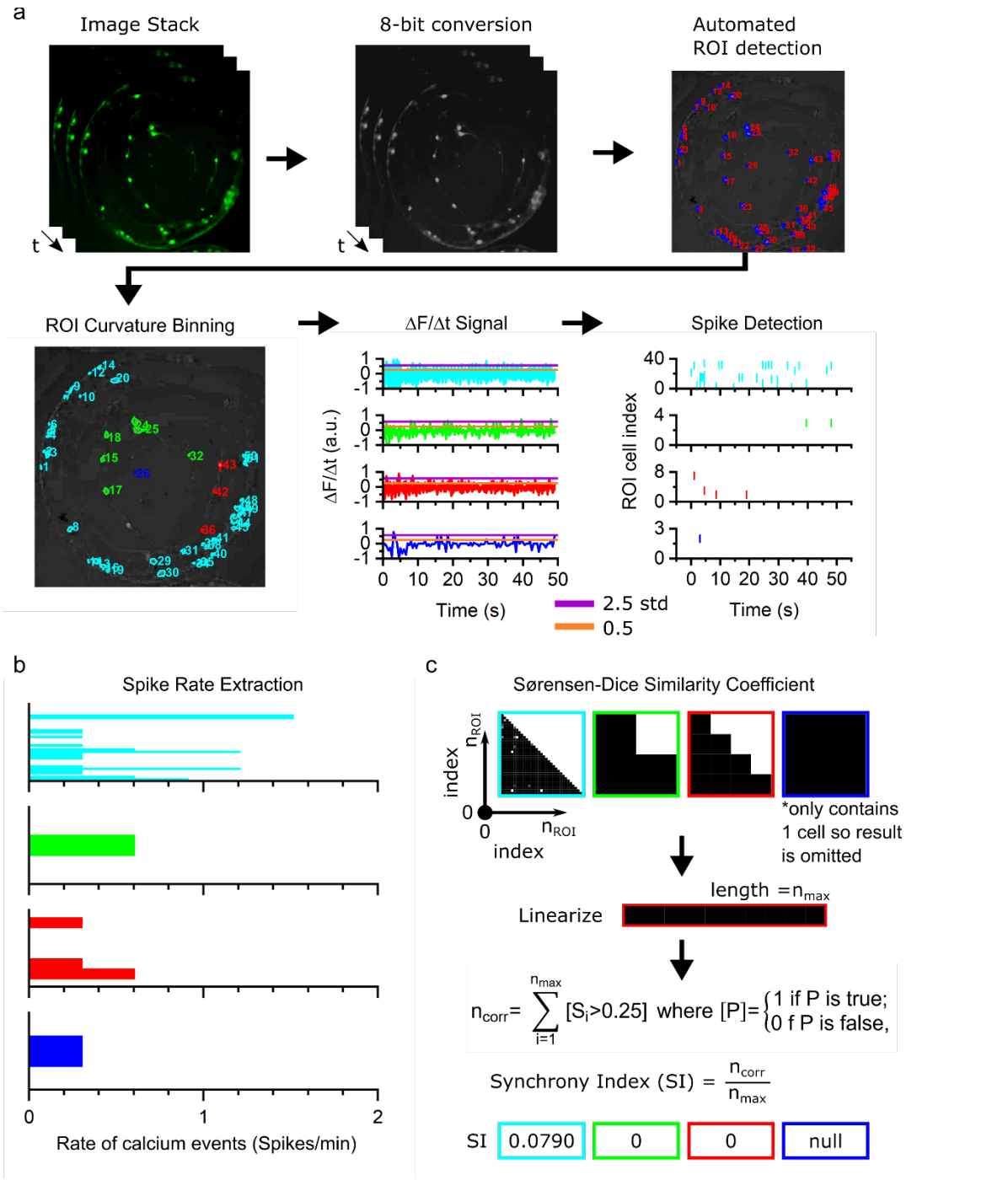

Figure S5: Image processing workflow to extract curvature-dependent transient calcium activity. (a) Selected multi-curvature pattern with temporal changes in fluorescent (12-bit, RGB) gets downsampled to gray-scale (8-bit). Automatic selection of a region of interest (ROI) based on single-cell body (n_{ROI}) segmentation is applied and subjected to a curvature mask specific to the pattern. For each specific ROI, changes in calcium fluorescence over time (ΔF/Δt) are captured. Spike events based on increasing calcium levels then get detected, and calcium events sorted based on distinct multi-curvature regions. (b) Bar plots show accumulated calcium events based on spike rate per minute associated with the distinct multi-curvature regions. (c) Synchronous calcium event activity within the neuronal network in each distinct curvature region is determined based on a comparison of correlated spikes (n_{corr}) over total number of spikes (n_{max}) using the Sørensen–Dice similarity coefficient and a synchronicity index (SI).

Summarizing curvature-dependent neuronal cell activity and growth behavior.

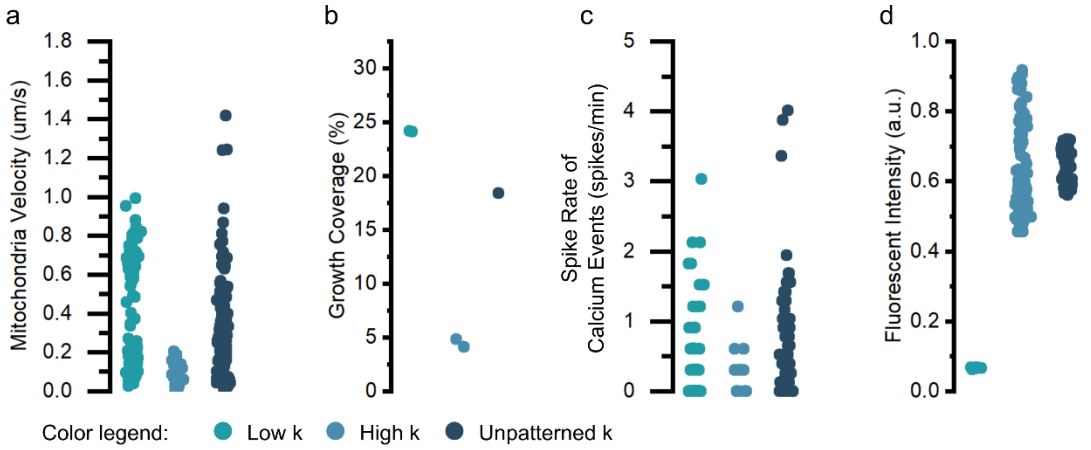

Figure S6: Scatter plots show curvature-dependent neuronal cell functionality and network behavior. (a) Velocity distribution of intracellularly moving mitochondria. (b) Cell growth coverage is based on seeded cell bodies in curvature grooves. (c) Transient calcium spike rate. (d) The fluorescent intensity scale shows static mean average calcium distribution. All data points are grouped based on low curvature ranges (low k, $0.003 < k < 0.01$), high curvature ranges (high k, $0.01 < k < 0.2$) and compared to unpatterned neuronal network growth (unpatterned k).

Supplementary video file.

An additional supplementary video file 1 (V1) is included, which shows calcium transients in Fluo4 AM loaded primary cortical neurons.

References:

1. N. Tanaka, T. Yamashita, A. Sato, V. Vogel and Y. Tanaka, *PLOS ONE*, 2017, **12**, e0173647.
2. A. Kunze, M. Giugliano, A. Valero and P. Renaud, *Biomaterials*, 2011, **32**, 2088-2098.
3. S. Kobel, M. Limacher, S. Gobaa, T. Laroche and M. P. Lutolf, *Langmuir*, 2009, **25**, 8774-8779.
4. Y. Ikegaya, G. Aaron, R. Cossart, D. Aronov, I. Lampl, D. Ferster and R. Yuste, *Science*, 2004, **304**, 559-564.
5. C. L. Beck, C. J. Hickman and A. Kunze, *Scientific Reports*, 2020, **10**, 12568.